



Pyrolysis of *Sedum plumbizincicola*, a zinc and cadmium hyperaccumulator: pyrolysis kinetics, heavy metal behaviour and bio-oil production

Daoxu Zhong¹ · Zhaoping Zhong¹ · Longhua Wu² ·
Kuan Ding¹ · Yongming Luo³ · Peter Christie²

Received: 15 October 2015 / Accepted: 6 March 2016 / Published online: 24 March 2016
© Springer-Verlag Berlin Heidelberg 2016

Abstract Appropriate disposal of hyperaccumulator biomass is a problem inhibiting the widespread use of phytoremediation technology. In the present study, kinetic analysis of the pyrolysis process of *Sedum plumbizincicola*, the behaviour of heavy metals and bio-oil composition were studied. The kinetic analysis of the pyrolysis process shows that activation energy (E) changed from 150 to 186 kJ mol⁻¹ and the frequency factor (A) changed from 1.34×10^{11} to 8.99×10^{15} s⁻¹. At temperatures of 450–750 °C more than 66.3 % of zinc (Zn) remained in the char. More than 87.6 % of the cadmium (Cd) was found in the bio-oil. Pyrolysis at 650 °C led to the highest yield of alkanes with low-oxygen compounds found in the bio-oil. Pyrolysis at 650 °C can likely offer a valuable processing method for *S. plumbizincicola* and recovery of Zn from the char and recovery of Cd from the bio-oil will be attempted in future research.

Keywords Hyperaccumulator · Pyrolysis · Heavy metals · Bio-oil · TG-DTG

Introduction

There are many anthropogenic sources of heavy metals that can contaminate soils. These include sewage sludges or urban composts, pesticides, fertilizers and car exhausts, as well as residues from metalliferous mining or smelting industries (Jones 1991). Heavy metals are highly persistent in soils with residence times in the order of hundreds or even thousands of years (Bradl 2004). Phytoremediation is the name given to the set of techniques which employ higher plants to sanitize contaminated environments (Salt et al. 1998). One of these techniques, phytoextraction, is used to clean up heavy metal-contaminated soils. Selected plant species remove metal compounds from the soil and accumulate them in their shoots. The technique is a modern environmentally sound and cost-efficient method for cleaning up metal-contaminated soils for which no suitable conventional treatment process has yet been found (Lewandowski et al. 2006; Chouchene et al. 2014). *S. plumbizincicola*, a zinc and cadmium hyperaccumulator, has a great capacity to extract Zn and Cd and has been demonstrated to successfully remediate Zn- and Cd-contaminated soils (Wu et al. 2013). *S. plumbizincicola* (Wu et al. 2013) has attracted growing interests because of its high dry matter yield (up to 12 t ha⁻¹), appropriate biomass characteristics, low nutrient requirements and positive environmental impact (Wu et al. 2013).

There are few published studies concerning pyrolysis of phytoextraction crop biomass. Most of the literature is focused on three goals: (1) to prevent heavy metals from being released into the environment; (2) to produce valuable

✉ Zhaoping Zhong
zzhong@seu.edu.cn

Daoxu Zhong
forever3159@163.com

Longhua Wu
lhwu@issas.ac.cn

¹ Key Laboratory of Energy Thermal Conversion and Control, Ministry of Education, and School of Energy and Environment, Southeast University, Nanjing 210096, Jiangsu, China

² Key Laboratory of Soil Environment and Pollution Remediation, Institute of Soil Science, Chinese Academy of Sciences, Nanjing 210008, Jiangsu, China

³ Key Laboratory of Coastal Zone Environmental Processes, Yantai Institute of Coastal Zone Research, Chinese Academy of Sciences, Yantai 264003, Shandong, China

pyrolysis oil that is free of heavy metals; and (3) to accumulate the heavy metals in the char/ash residue (hereafter described as ‘char’) (Lievens et al. 2009; Stals et al. 2010; Han et al. 2013; Cheng 2014; Yang et al. 2014). It has been found that both condensable and non-condensable pyrolysis (623 K) fractions of both contaminated willow stems and leaves contain no detectable amounts of Cd, Cu or Pb but very small amounts of Zn (<5 ppm) are found in the condensable pyrolysis fraction (623 K) (Lievens et al. 2009). Pilot scale pyrolysis of synthetic hyperaccumulator biomass has also been demonstrated. In this context, the term ‘synthetic’ refers to the authors of Ref. (Koppolu et al. 2004) applying a laboratory process to obtain the heavy metals taken up by the originally uncontaminated biomass. When both stems and leaves were pyrolysed in a laboratory-scale semi-continuous reactor it was found that very low levels of metals occurred in pyrolysis oil produced at 623 K (Cu and Zn < 5 ppm; Cd and Pb < 1 ppm) with almost all of the metals accumulated in the char/ash residue (Stals et al. 2010). Using three types of biomass (switchgrass, hardwood and softwood) through either fast pyrolysis in a fluidized-bed reactor (at 500 °C) or slow pyrolysis (at 500 and 700 °C) it was found that most of the Zn²⁺ and Cu²⁺ were adsorbed onto the biochars and the activated carbon (Han et al. 2013). After rapid pyrolysis of birch and sunflower at low temperature it was found that heavy metals were concentrated in the ash/char fraction and Cd compounds were more susceptible to volatilization at 673 K (Lieves et al. 2008). In fast, pyrolysis of heavy metal-contaminated willow with high concentrations of Cd, Cu, Pb and Zn the two pyrolysis fractions (at an operational temperature of 623 K), i.e. bio-oil/tar and gas, were both free of heavy metals. Some small differences in the types and amounts of organic compounds are found in the bio-oil and gaseous fractions (Lievens et al. 2009). Another approach for processing of phytoremediation crops is based on conversion into bioenergy using different energy-recovery techniques (Keller et al. 2005). Because pyrolysis effectively destroys the organic portion of the plant biomass it is implicitly assumed that the ultimate fate of the metals and the energy recovery are from the bio-oil. During reduction in the thermal process of *Sedum plumbizincicola* both Pb and Cd formed metal complexes such as Ca0.75Cd0.25O and Pb2O3.333 or their mixtures and more of the bottom ash Zn under the reducing conditions was present as pure metal, crystalline oxides, sulphides or complex compounds combined with other metals (Zhong et al. 2015). However, to our knowledge, there is little information available about the pyrolysis kinetics of hyperaccumulator biomass, the heavy metals in bio-oils, or the composition of the bio-oils.

In the present study, thermogravimetric analysis was used to investigate the pyrolysis behaviour of *S. plumbizincicola* at three different heating rates and find the

distributed activation energies(*E*), frequency factor(*A*) and coefficients corresponding to different mass conversions. *S. Plumbizincicola* was also pyrolysed at 450, 550, 650 and 750 °C in a laboratory-scale horizontal quartz tube with 15 g of biomass per experiment. The bio-oil composition was characterized using pyrolysis–gas chromatography–mass spectroscopy (Py–GC–MS).

Materials and methods

Materials

S. plumbizincicola biomass was collected from the mine area where it was originally found at a Pb/Zn mine in Chun'an City, Zhejiang Province, East China. The biomass pyrolysis test was carried out in a horizontal quartz tube. The proximate and ultimate analysis results for *S. plumbizincicola* are shown in Table 1. The content of nitrogen, volatile matter and ash were large, but the sulphur concentration was low. The elemental composition (mg kg⁻¹) of *S. plumbizincicola* comprised 9838 ± 289 (Zn), 560 ± 6 (Cd), 62.5 ± 3.7 (Pb), 77.6 ± 1.7 (Cu), 45.4 ± 6.0 (Cr), 642 ± 46 (Fe), 84.8 ± 6.9 (Na), 13976 ± 543 (Al), 61886 ± 805 (Ca) and 1135 ± 15 (Cl), respectively, and the SiO₂ content was 850 mg kg⁻¹. The ash concentration was 8.17 %.

Py–GC–MS and oil product analysis

Pyrograms were obtained by interfacing the pyrolyser (Model 5200, CDS, Oxford, PA) to the instrument used for GC–MS analysis (Model 7890A-5975C, Agilent, Santa Clara, CA). Portions (0.50 mg) of the biomass samples were pyrolysed at 450, 550, 650 and 750 °C for 10 s, respectively, with a heating rate of 20°Cms⁻¹. The temperatures of the injector and of the GC–MS interface were 270 and 290 °C, respectively. GC separation was achieved on an Agilent HP-5 ms (30 m × 0.25 mm × 0.25 μm). The following temperature program was set up: isothermal

Table 1 Proximate and ultimate analysis of *S. plumbizincicola* biomass

Proximate analysis		Ultimate analysis	
Component	Result	Component	Result
Ash (%)	8.17	C (%)	40.2
Volatile carbon (%)	66.82	H (%)	6.0
Fixed carbon (%)	15.50	N (%)	1.1
Moisture (%)	9.51	S (%)	0.1
		O (%)	45.3
		Calorific value (J/g)	15188

conditions at 50 °C for 1 min, up to the final temperature of 290 °C with a rate increase of 8.0 °C min⁻¹ and isothermal conditions at 290 °C for 2 min. Ultrapure grade He was the carrier gas and its flow rate was 1.0 mL min⁻¹. The injection mode was split (split ratio = 8, split flow = 10 mL min⁻¹). Mass spectrometer conditions were as follows: 35–550 m/z, range of analysis: 0.49 s, scan event time; 3, number of microscans; 25 ms, max ion time. The ion source was at 230 °C and positive ions were analysed. The NIST reference library of known organic ingredients was used to determine the chemical composition of the pyrolysis products.

Thermogravimetric analysis

A TG-DTG Evolution 16 analyser (Setaram, Caluire, France) was used to study the evolution of weight and volatile matter of *S. plumbizincicola* biomass from Chunn'an during pyrolysis. About 10 mg of the sample was tested at ambient temperature to 800 °C and the heating rate was set at 10, 30 and 50 °C min⁻¹. Nitrogen was used as the inert gas and the sampling time was 1 s per point.

Kinetic analysis using DAEM

The distributed activation energy model (DAEM) has been widely used to analyse complex reaction systems (Wang et al. 2008; Shen et al. 2011). In the present study, thermal conversion process of *S. plumbizincicola* under an inert atmosphere is composed of a set of irreversible single (first-order) reactions occurring successively (Cheng et al. 2015; Li et al. 2013). The model is expressed as follows (Miura 1995):

$$\ln(\beta/T^2) = \ln(AR/E) + 0.6075 - E/RT. \quad (1)$$

Equation (1) develops a linear relationship between $\ln(\beta/T^2)$ and $(1/T)$ with the slope $(-E/R)$. Consequently, the

activation energy for the reaction can be determined by the slope of the linear-fitting curve from the correlated experimental data, while the pre-exponential factor A is estimated from the intercept (Miura 1995).

Experimental facility

The experimental facility is shown in Fig. 1 and contained a high-pressure gas source (N_2), a flow control valve and metre, a horizontal quartz tube with a surrounding electrically heated furnace, and a flue gas absorption device. The horizontal quartz tube had an inner diameter of 45 mm and a length of 1000 mm of which 400 mm was in the temperature controlled reaction zone heated and controlled by the electrical furnace from 100 to 1100 °C. All flue samples were collected in each experiment. A glass fibre filter plugged the joint between the quartz tube and the condenser pipe. About 15 grams of *S. plumbizincicola* powder were placed in each of four dried and weighed quartz-weighing boats and transferred into the centre of the quartz tube which was pre-heated to the desired temperature and was purged with N_2 in advance for about 10 min. The gas flow was introduced into the quartz tube before the start of the experiments. After each experiment the absorption bottles containing 5 % HNO_3 + 10 % H_2O_2 solution were removed and replaced with another set of bottles to dispose of the exhaust gas. The heating source was cut off. After the tube furnace was sufficiently cooled the bottom ash was carefully taken out, allowed to cool to room temperature, weighed and sealed in a sampling bag.

Determination of heavy metals

Samples of bio-oil, tar and char were digested with a solution of HNO_3 , $HClO_4$ and HF (3:2:1 HNO_3 : $HClO_4$:HF by volume) for determination of Cd, Zn and Pb. The Zn and Pb concentrations were determined by flame atomic

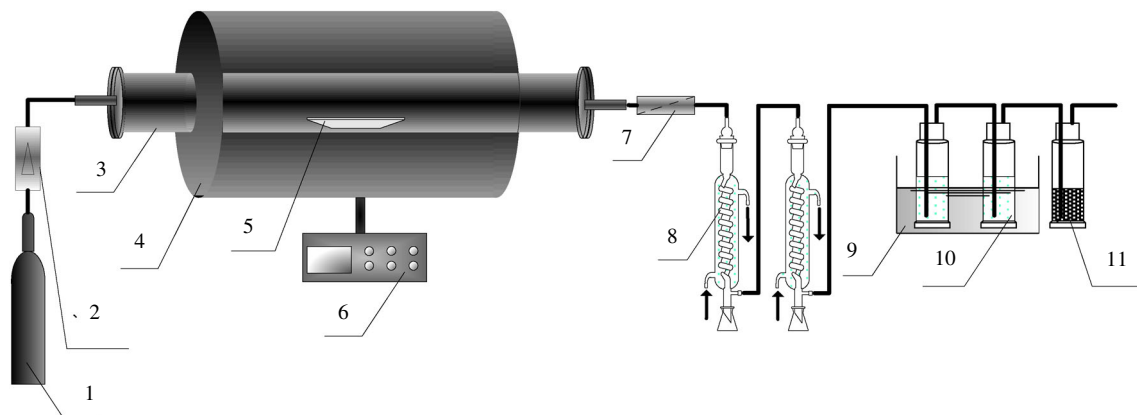


Fig. 1 Schematic diagram of the setup of the horizontal tube furnace. NB 1 high-pressure N_2 ; 2 flow metre, 3 horizontal quartz tube, 4 quartz boat, 5 electrically heated furnace, 6 temperature controller, 7

fibre-glass filter, 8 condenser tube, 9 iced-water bath, 10 absorption solution 1(5 % HNO_3 + 10 % H_2O_2), 11 silica gel

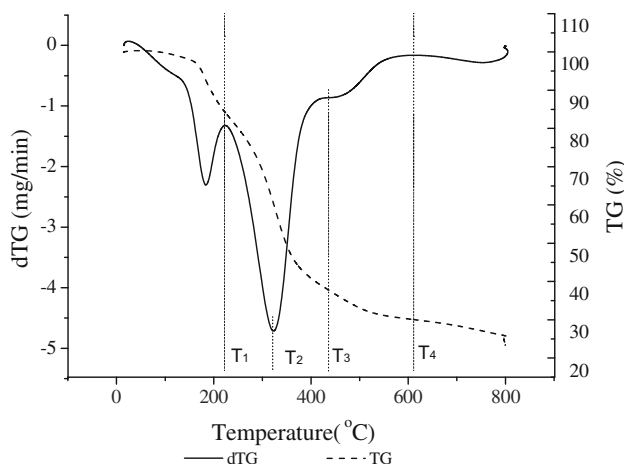


Fig. 2 Typical TG-DTG curves of *S. plumbizincicola* at a heating rate of $50\text{ }^{\circ}\text{C min}^{-1}$

Table 2 The activation energies obtained at different conversion rates

m/m ₀	E/kJ mol ⁻¹	A/S ⁻¹	R ²
0.1	150.25	1.19×10^{15}	0.9446
0.2	150.76	2.37×10^{14}	0.9176
0.3	155.32	2.03×10^{14}	0.9049
0.4	165.11	6.83×10^{14}	0.9232
0.5	176.43	3.23×10^{15}	0.9450
0.6	185.61	8.99×10^{15}	0.9645
0.7	183.99	2.11×10^{15}	0.9965
0.8	170.00	1.56×10^{13}	0.8575
0.9	158.79	1.34×10^{11}	0.8856
Average	166.25		

absorption spectrophotometry (SpectraA 220FS, Varian, Palo Alto, CA). The solution Cd concentration was determined with a Varian SpectraA 220Z spectrophotometer using a graphite furnace.

Results and discussion

Kinetic analysis of the pyrolysis process

Stage II of the pyrolysis process of *S. plumbizincicola* (Zhong et al. 2015) was chosen for calculating the activation energy of *S. plumbizincicola* using DAEM model based on three different heating rates ($\beta = 10, 30, \text{ or } 50\text{ K min}^{-1}$) (Fig. 2). The calculated kinetic parameters and deviation values were obtained and the results are shown in Table 2. Fig. 3 shows a good linear relationship (linear correlation coefficients >0.85) between the arrhenius plot of $\ln(\beta/T_2)$) and $1/T$ (Table 3). The E values changed from 150.25 to 185.61 kJ mol⁻¹ and the values of

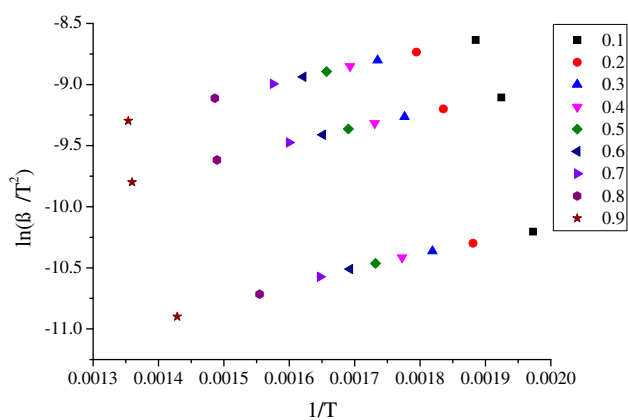


Fig. 3 Plots for determining activation energy at different conversion rates of stage II

A change from 1.34×10^{11} to $8.99 \times 10^{15}\text{ s}^{-1}$. The average E value of *S. plumbizincicola* lower than other types of biomass (Giuntoli et al. 2009; Cheng et al. 2015), possibly because the chemical composition of individual species plays a fundamental role in determining the kinetics or may be associated with the presence and absence of mineral content in various biomass materials (Giuntoli et al. 2009; Cheng et al. 2015).

Distribution of pyrolysis products from *S. plumbizincicola*

The distribution of products from pyrolysis of *S. plumbizincicola* is shown in Fig. 4. The bio-oil yield increased from 22.01 wt% at 450 °C to 31.7 wt% at 650 °C and decreased to 15.9 wt% at 750 °C. The tar yield increased to 6.34 % at 650 °C and decreased to 3.19 wt% at 750 °C. Char yield was found to decrease from 32.43 to 22.49 wt% when the temperature increased from 450 to 750 °C. The yields of gas remained nearly constant up to 650 °C then increased significantly at 750 °C. The results are similar to those of Xue et al. (2015), who reported that char decreased with the char mainly converted to bio-oil during pyrolysis at temperatures up to about 650 °C. However, pyrolysis at even higher temperatures caused the cracking of pyrolysis-oil to gas.

Behaviour of heavy metals during pyrolysis

Temperature has a significant impact on the heavy metal volatilization process. Increasing temperature can enhance vapourization by raising the vapour pressure of metal chlorides and enhancing the rates of diffusion (Sun et al. 2004; Liu et al. 2010).

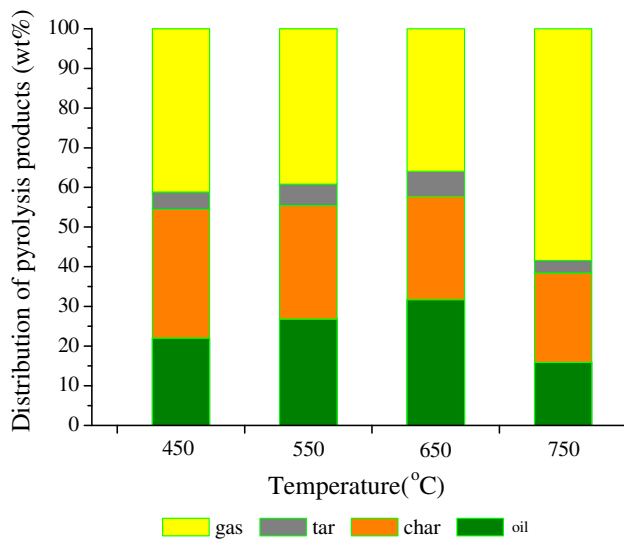
Heavy metals in the gas were not detected. The recovery of heavy metals in pyrolysis oil, tar and char were calculated from the total amount of metal available in the

Table 3 Yields of the main chemical compounds in the bio-oil at different temperatures (°C)

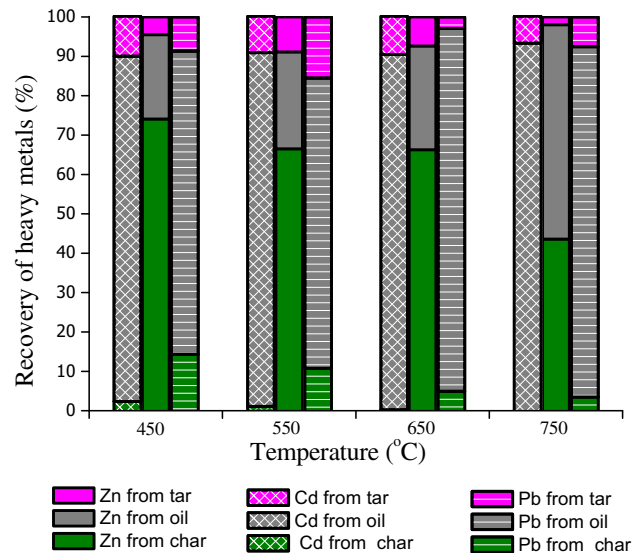
Temperature	450	550	650	750
Alcohol				
Cyclobutanol	6.465	1.852		1.628
3,7,11,15-Tetramethyl-2-hexadecen-1-ol	2.387			
Ethanol, 2-(9-octadecenoxy)-, (Z)-	0.549	0.999	0.178	2.224
2,2,4-Trimethyl-3-(3,8,12,16-tetramethyl-heptadeca-3,7,11,15-tetraenyl)-cyclohexanol	0.476	1.752		
Others	1.513	0.775	3.634	5.474
Aromatics				
2-Methoxy-4-vinylphenol	0.951			
3',8,8'-Trimethoxy-3-piperidyl-2,2'-binaphthalene-1,1',4,4'-tetrone	0.362			
Benzyl methyl ketone			4.348	
Toluene				4.976
Phenol				2.358
Phenol, 4-methyl-			0.822	2.046
Styrene				2.192
Others	0.281		0.928	8.152
Aldehydes				
Furfural	3.758			10.51
Butanal, 3-hydroxy-	0.655			
Acetaldehyde			2.434	
Butanal, 3-hydroxy-			1.333	
Butanodial			0.633	
3-Cyclopentene-1-acetaldehyde, 2-oxo-			3.301	
Acids				
Acetic acid	5.578	15.60	22.34	9.972
Hexadecenoic acid	22.70	3.608		
Octadecanoic acid	22.92			
Oleic acid	7.989	0.969		6.779
Others	5.777		2.184	8.997
Saccharides				
πD-Glucopyranoside, O-πD-glucopyranosyl-(1.fwdarw.3)-πD-fructofuranosyl	1.921			
πD-Glucopyranose, 1,6-anhydro-		6.346		
Phenyl-πD-glucoside			1.208	
Others		2.110	1.486	
Ketones				
2-Propanone, 1-hydroxy-	1.982	8.488	5.458	3.496
2-Hexanone, 6-hydroxy-	1.100			0.688
Ethanone, 1-(1-cyclohexen-1-yl)-	1.065	0.751	0.912	1.375
1-Propen-2-ol, acetate		10.87		
2,3-Butanedione		4.531	2.721	2.941
13,27-Cycloursan-3-one		1.075		2.958
Others	1.216	12.28	9.551	4.523
Alkanes				
Nonacosane	4.562			4.265
Heptacosane	2.594	1.962		1.609
17-Pentatriacontene		2.773	0.431	
Ethane-1,2-diimine, N,N'-diamino-			9.679	
Tetratetracontane			4.167	
Tetratetracontane			3.860	

Table 3 continued

Temperature	450	550	650	750
Hexacosane				2.766
Butane				2.746
D-Limonene				1.537
Others			3.061	0.662
Heterocyclics				
Aziridine, 2-methyl-3-(1-methylethyl)-1-(2-propenyl)-, trans-	1.336	0.458	0.417	
2-Vinyl-9-[3-deoxy- π d-ribofuranosyl]hypoxanthine	1.795	3.807	2.845	
1,4:3,6-Dianhydro- π d-glucopyranose		1.381		
Pyrrole				1.181
3,8-Dioxatricyclo[5.1.0.0(2,4)]octane, 4-ethenyl-	0.693			
Others		1.674		
Esters				
Docosanoic acid, 1,2,3-propanetriyl ester	0.409			
sec-Butyl nitrite			2.168	
2-Propanone, 1-(acetyloxy)-		2.383		
Ethanol, 2-nitro-, propionate (ester)		1.205	2.008	
2-Butanone, 1-(acetyloxy)-		3.866		
Acetic acid, 9,9-dioxo-9-thiabicyclo[3.3.1]non-6-en-2-yl ester			2.130	
7-Isopropylidene-5-methyl-2,3-diazabicyclo[2.2.1]hept-5-ene-2,3-dicarboxylic acid, diethyl ester				1.307
9-Tetradecen-1-ol, acetate, (E)-	1.113	0.585		
[1,1'-Bicyclopentyl]-2-octanoic acid, 2'-hexyl-, methyl ester		1.800		
Cholest-22-ene-21-ol, 3,5-dehydro-6-methoxy-, pivalate		2.232		
Oleic acid, eicosyl ester				1.177
Others	0.688	2.319	3.883	1.463

**Fig. 4** Distribution of pyrolysis products from *S. plumbizincicola*

biomass feedstock (Table 1). The recoveries of heavy metals are depicted in Fig. 5. The recoveries of Cd, Pb and Zn from char decreased with increasing temperature. At temperatures 450–750 °C the major portion of Zn

**Fig. 5** Recovery of heavy metals during pyrolysis of *S. plumbizincicola*

(>43.6 %) remained in the char while 54.4 % was found in the oil at 750 °C. The major portions of Pb (>73.6 %) and Cd (>87.6 %) were vapourized during pyrolysis and were

found in the oil. Only a minority of Pb (3.50–14.3 %) and Cd (0.02–2.16 %) was found in the char. Therefore, it can be concluded that Pb and Cd were mainly volatilized at reactor temperatures >450 °C and condensed in the oil. Most of the Zn was volatilized when the temperature was >750 °C. Preliminary demonstration of laboratory-scale (3 g batch⁻¹) fast pyrolysis (30 K min⁻¹ heating rate) in a quartz tubular reactor also shows Cd being volatized at elevated temperatures. Zn, Pb and Cu are much less prone to volatilization and remain in the char (Lieves et al. 2008). The retention of heavy metals in the char leads to increased concentrations. Char mass is typically only 20–35 % of the original mass, depending on the biomass feedstock (Fahmi et al. 2008).

Bio-oil composition

Bio-oil may consist of more than 300 organic compounds. It is an easily transportable source of chemicals and it has an energy content higher than that of biomass (Bulushev and Ross 2011). The chemical composition of bio-oils is very complex because they are mainly composed of a mixture of oxygenated compounds formed by the fragmentation and depolymerization reactions of cellulose, hemicellulose and lignin by their rapid heating (Mohan et al. 2006; Garcia-Perez et al. 2007; Stelmachowski 2011).

The bio-oil compounds have been grouped in Table 3 according to their functional groups together with the main individual compounds. These results correspond to more than 55 compound identified that account for >90 % of the whole bio-oil. These oxygenated compounds (phenols, cyclopentenones, furans, open chain Ketones, aldehydes, carboxylic acids and monosaccharides) make the bio-oil unstable and reduce miscibility with hydrocarbons and the heating value (Bridgwater 2012; Alper et al. 2015). Moreover, the heterocyclic compounds of the bio-oil make it viscous and easy to polymerize.

As observed in Table 3, the main organic compounds in the bio-oil are acids. Py-GC-MS studies show that at a low temperature (450 °C) the content of bio-oil acids was 65.0 % (acetic acid 5.6, 22.7 % stearic acid and oleic acid 30.9 %, respectively). The formation of acids decreased with increasing pyrolysis temperature and made up 20.2–25.7 % of the GC-MS chromatograms, were formed in different quantities during pyrolysis. The group of acids with 18 carbon atoms (octadecanoic acid and oleic acid) are the most common acids in the pyrolysis products of *S. plumbizincicola* at 450 °C. Oleic acid was not found when temperature was 650 °C. The main compound in this group is Octadecanoic acid (22.3 %, at 650 °C) and the group of acids with 18 carbon atoms (30.9 % at 450 °C). The presence of acetic acid is specifically attributed to the deacetylation of hemicelluloses (Weres et al. 1988). The

presence of these carboxylic acids is responsible for the strong acidity of the bio-oil (pH 2.0–3.0). They can cause corrosion in downstream processing when equipment is made of low quality materials (e.g. carbon steel).

Ketones make up the second major organic group in the bio-oil and they peak at 550 °C (38.0 wt%). This chemical family is made up of two kinds of Ketones: cyclopentenones (ethanone, 1-(1-cyclohexen-1-yl)-r) and open-chain Ketones (2-propanone, 1-hydroxy-r). As observed in Table 3, cyclopentenone increased with temperature and increased to 4.33 wt% in the liquid. 26.9 wt% of chain Ketones were found at 550 °C and decreased with increasing temperature. Ketones are formed by condensation reactions of the carbohydrate-derived fraction and decomposition of the miscellaneous oxygenates, sugars and furans (Mohan et al. 2006).

Aromatics comprise another important group and are formed in the decomposition of *S. plumbizincicola* above 450 °C, and their yields increase considerably at 750 °C (19.7 wt%). At very high temperatures, dehydrogenation/aromatization reactions can eventually lead to larger polynuclear aromatic hydrocarbons and, eventually, increases in carbonization (Alvarez et al. 2014). These results are consistent with the lignin pyrolysis mechanism proposed by Demirbas (Elliott 1986), i.e. the monomolecular dissociation of guaiacols into the corresponding radicals (catechols and cresols) at higher temperatures. Currently, phenol is synthesized from the partial oxidation of benzene, according to the cumene process, or the Raschig–Hooker process. These typical synthesis methods are usually very complex and the phenol produced by these methods is expensive.

The aldehydes in the pyrolysis products make up 10.5 % (at 750 °C) of the GC-MS identified *S. plumbizincicola* pyrolysis products in the bio-oil mixture. The main aldehyde in the bio-oil is furfural which reaches its maximum concentration in bio-oil produced at higher temperatures. The furfural is attributed to the ring-open and rearrangement reactions of the xylan unit (Shafizad et al. 1972). Furfural (FF) is regarded as a typical ring-containing product in the bio-oil (Shafizad et al. 1972). The yield of furfural has been found to increase as the temperature rises, i.e. high temperatures favour the formation of furfural (Table 3). An earlier study (Shafizad et al. 1972) showed that the addition of zinc chloride also facilitates the formation of furfural from the hemicellulose pyrolysis. It is achieved through the concerted cleavage of the bond between oxygen and the C-5 position and ring forming between C-2 and C-5 positions on the xylan unit along with a free radical of H. Two new chemical pathways are proposed for the production of furfural here. These yields are much higher than those corresponding to other bio-oils derived from wood which are usually below 0.5 wt% (Qiang et al. 2008).

Alkanes such as nonacosane, heptacosane, tetratetracontane and butane were detected with total contents of 4.76–21.2 % and peaks at 650 °C. These alkanes are possibly generated from the conversion of unsaturated fatty acids in algal cells (Zhou et al. 2010) or dehydration of alcohols and ethers (Weres et al. 1988).

Alcohols make up 11.4 % (at 450 °C) and 9.32 % (at 750 °C), improve the homogeneity, decrease the viscosity and density, lower the flash point and increase the heating value of the pyrolysis liquids.

Among the chemical compounds identified, the content of saccharides (8.46 wt% at 550 °C) and the content of acetic acid (15.6 wt% at 550 °C) were higher than other biomass components such as corn stalk, fir wood, rice husk and bagasse and the ketone content of 38.00 wt% at 550 °C was also high compared with most other biomass materials (Lu et al. 2011a, b). Only 0.36 wt% of aromatics were found at 550 °C. The low aromatic content may due to the low lignin content and increased with increasing temperature because alkyl groups cleave from aromatic compounds as the temperature increases (Mohan et al. 2006). Eventually, the aromatic compounds condense into polycyclic aromatic hydrocarbons (PAHs) at the higher temperatures (Mohan et al. 2006). *S. plumbizincicola* can be pyrolysed at 650 °C with the highest yield of alkanes and esters with a low yield of acids.

Conclusions

DAEM was used in kinetic analysis and provided reasonable fits to the experimental data. The activation energy of *S. plumbizincicola* ranged from 146.4 to 232.4 kJ mol⁻¹, and the frequency factor (*A*) values changed greatly corresponding to *E* values at different mass conversions. Heavy metals in the gas were no detected. At temperatures of 450–650 °C, the major portion of Zn (>43.6 %) remained in the char, while 54.4 % was found in the oil at 750 °C. The major portions of Pb (>73.6 %) and Cd (>87.6 %) were vapourized during pyrolysis and found in the oil. The main components of the pyrolysis oils were acids (at 450 °C) which decreased with increasing pyrolysis temperature. With pyrolysis at 650 °C, the highest yields were obtained of alkenes with low levels of oxygenated compounds in the bio-oil. Pyrolysis at 650 °C with heavy metals cleaning technologies (cyclone for collecting tar/char and with spray tower for collecting and cooling bio-oil) can likely offer a valuable processing method for *S. plumbizincicola*. Recovery of Zn from the char and that of Cd from the bio-oil will require further research.

Acknowledgments We thank the National Natural Science Foundation of China (41325003, 51276040 and U1361115) and the

National High Technology Research and Development (863) Program of China (2012AA101402-2) for financial support.

References

- Alper K, Tekin K, Karagoz S (2015) Pyrolysis of agricultural residues for bio-oil production. *Clean Technol Environ Policy* 17(1):211–223
- Alvarez J, Lopez G, Amutio M, Bilbao J, Olazar M (2014) Bio-oil production from rice husk fast pyrolysis in a conical spouted bed reactor. *Fuel* 128:162–169
- Bradl HB (2004) Adsorption of heavy metal ions on soils and soils constituents. *J Colloid Interface Sci* 277(1):1–18
- Bridgwater AV (2012) Review of fast pyrolysis of biomass and product upgrading. *Biomass Bioenergy* 38:68–94
- Bulushev DA, Ross JRH (2011) Catalysis for conversion of biomass to fuels via pyrolysis and gasification: a review. *Catal Today* 171(1):1–13
- Cheng CC (2014) Effects of municipal sludge and wheat straw pyrolysis on changes of shapes of heavy metals. *Asian J Chem* 26(1):21–24
- Cheng ZC, Wu WX, Ji P, Zhou XT, Liu RH, Cai JM (2015) Applicability of Fraser-Suzuki function in kinetic analysis of DAEM processes and lignocellulosic biomass pyrolysis processes. *J Therm Anal Calorim* 119(2):1429–1438
- Chouchene A, Jeguirim M, Trouve G (2014) Biosorption performance, combustion behavior, and leaching characteristics of olive solid waste during the removal of copper and nickel from aqueous solutions. *Clean Technol Environ Policy* 16(5):979–986
- Elliott DC (1986) Analysis and comparison of biomass pyrolysis/gasification condensates: Final report. Other Information: portions of this document are illegible in microfiche products. Original copy available until stock is exhausted: Medium: ED; Size, 100
- Fahmi R, Bridgwater A, Donnison I, Yates N, Jones JM (2008) The effect of lignin and inorganic species in biomass on pyrolysis oil yields, quality and stability. *Fuel* 87(7):1230–1240
- Garcia-Perez M, Chaala A, Pakdel H, Kretschmer D, Roy C (2007) Characterization of bio-oils in chemical families. *Biomass Bioenergy* 31(4):222–242
- Giuntoli J, Arvelakis S, Spliethoff H, de Jong W, Verkooijen AHM (2009) Quantitative and Kinetic Thermogravimetric Fourier Transform Infrared (TG-FTIR) study of pyrolysis of agricultural residues: influence of different pretreatments. *Energy Fuels* 23:5695–5706
- Han YX, Boateng AA, Qi PX, Lima IM, Chang JM (2013) Heavy metal and phenol adsorptive properties of biochars from pyrolyzed switchgrass and woody biomass in correlation with surface properties. *J Environ Manag* 118:196–204
- Jones KC (1991) Contaminant trends in soils and crops. *Environ Pollut* 69(4):311–325
- Keller C, Ludwig C, Davoli F, Wochele J (2005) Thermal treatment of metal-enriched biomass produced from heavy metal phytoextraction. *Environ Sci Technol* 39(9):3359–3367
- Koppolu L, Prasad R, Clements LD (2004) Pyrolysis as a technique for separating heavy metals from hyperaccumulators. Part III: pilot-scale pyrolysis of synthetic hyperaccumulator biomass. *Biomass Bioenergy* 26(5):463–472
- Lewandowski I, Schmidt U, Londo M, Faaij A (2006) The economic value of the phytoremediation function: Assessed by the example of cadmium remediation by willow (*Salix* ssp). *Agric Syst* 89(1):68–89
- Li LL, Wang G, Wang SY, Qin S (2013) Thermogravimetric and kinetic analysis of energy crop Jerusalem artichoke using the

- distributed activation energy model. *J Therm Anal Calorim* 114(3):1183–1189
- Lievens C, Carleer R, Cornelissen T, Yperman J (2009) Fast pyrolysis of heavy metal contaminated willow: influence of the plant part. *Fuel* 88(8):1417–1425
- Lieves C, Yperman J, Vangronsveld J, Carleer R (2008) Study of the potential valorisation of heavy metal contaminated biomass via phytoremediation by fast pyrolysis: Part I. Influence of temperature, biomass species and solid heat carrier on the behaviour of heavy metals. *Fuel* 87(10–11):1894–1905
- Liu J, Falcoz Q, Gauthier D, Flamant G, Zheng CZ (2010) Volatilization behavior of Cd and Zn based on continuous emission measurement of flue gas from laboratory-scale coal combustion. *Chemosphere* 80(3):241–247
- Lu Q, Dong C-Q, Zhang X-M, Tian H-Y, Yang Y-P, Zhu X-F (2011a) Selective fast pyrolysis of biomass impregnated with ZnCl₂ to produce furfural: analytical Py-GC/MS study. *J Anal Appl Pyrol* 90(2):204–212
- Lu Q, Wang Z, Dong C-Q, Zhang Z-F, Zhang Y, Yang Y-P, Zhu X-F (2011b) Selective fast pyrolysis of biomass impregnated with ZnCl₂: furfural production together with acetic acid and activated carbon as by-products. *J Anal Appl Pyrol* 91(1):273–279
- Miura K (1995) A new and simple method to estimate f(E) and K(0)(E) in the distributed activation-energy model from 3 sets of experimental-data. *Energy Fuels* 9(2):302–307
- Mohan D, Pittman CU, Steele PH (2006) Pyrolysis of wood/biomass for bio-oil: a critical review. *Energy Fuels* 20(3):848–889
- Qiang L, Xu-Lai Y, Xi-Feng Z (2008) Analysis on chemical and physical properties of bio-oil pyrolyzed from rice husk. *J Anal Appl Pyrol* 82(2):191–198
- Salt DE, Smith RD, Raskin I (1998) Phytoremediation. *Annu Rev Plant Physiol Plant Mol Biol* 49:643–668
- Shafizad F, McGinnis GD, Philpot CW (1972) Thermal-degradation of xylan and related model compounds. *Carbohydr Res* 25(1):23–33
- Shen DK, Gu S, Jin BS, Fang MX (2011) Thermal degradation mechanisms of wood under inert and oxidative environments using DAEM methods. *Bioresour Technol* 102(2):2047–2052
- Stals M, Thijssen E, Vangronsveld J, Carleer R, Schreurs S, Yperman J (2010) Flash pyrolysis of heavy metal contaminated biomass from phytoremediation: influence of temperature, entrained flow and wood/leaves blended pyrolysis on the behaviour of heavy metals. *J Anal Appl Pyrol* 87(1):1–7
- Stelmachowski M (2011) Utilization of glycerol, a by-product of the transesterification process of vegetable oils: a review. *Ecol Chem Eng S-Chemia I Inżynieria Ekologiczna S* 18(1):9–30
- Sun LS, Abanades S, Lu JD, Flamant G, Gauthier D (2004) Volatilization of heavy metals during incineration of municipal solid wastes. *J Environ Sciences-China* 16(4):635–639
- Wang G, Li W, Li BQ, Chen HK (2008) TG study on pyrolysis of biomass and its three components under syngas. *Fuel* 87(4–5):552–558
- Weres O, Newton AS, Tsao L (1988) Hydrous pyrolysis of alkanes, alkenes, alcohols and ethers. *Org Geochem* 12(5):433–444
- Wu LH, Liu YJ, Zhou SB, Guo FG, Bi D, Guo XH, Baker AJM, Smith JAC, Luo YM (2013) Sedum plumbizincicola X.H. Guo et S.B. Zhou ex L.H. Wu (Crassulaceae): a new species from Zhejiang Province, China. *Plant Syst Evol* 299(3):487–498
- Xue Y, Zhou S, Brown RC, Kelkar A, Bai XL (2015) Fast pyrolysis of biomass and waste plastic in a fluidized bed reactor. *Fuel* 156:40–46
- Yang FS, Zhang M, Zhou AN, Lin MQ, Wei BL (2014) Research on immobilization of heavy metals in sludge by pyrolysis. *Environ Eng, Pts 1–4.* Li I, Xu Q, Ge H, Stafa-Zurich, Trans Tech Publications Ltd. 864–867: 1745–1749
- Zhong DX, Zhong ZP, Wu LH, Xue H, Song ZW, Luo YM (2015) Thermal characteristics and fate of heavy metals during thermal treatment of *Sedum plumbizincicola*, a zinc and cadmium hyperaccumulator. *Fuel Process Technol* 131:125–132
- Zhou D, Zhang LA, Zhang SC, Fu HB, Chen JM (2010) Hydrothermal Liquefaction of Macroalgae Enteromorpha prolifera to Bio-oil. *Energy Fuels* 24:4054–4061